Table 2 Baseline Characteristics

	Acute Myocardial Infarction n = 45	Unstable Angina n = 27	P
Age, yr	65.1 ± 10.4	62.6 ± 9.7	0.37
Male, Female	31 (68.8)	17 (65.9)	0.39
Diabetes Mellitus	15 (33.3)	6 (22.2)	0.23
Hypertension	22 (51.1)	14 (51.8)	0.49
Hyperlipidemia	23 (53.1)	13 (48.1)	0.49
Serum Lipid Levels			
Total Cholesterol, mg/dl	200.3 ± 36.7	185.1 ± 31.7	0.13
Triglycerides, mg/dl	147.3 ± 138.0	117.6 ± 58.1	0.33
High-density Lipoprotein Cholesterol, mg/dl	43.8 ± 12.7	43.8 ± 12.7	0.28
Smoking History	33 (75.0)	16 (59.2)	0.16
Body Mass Index, Kg/mm^2	23.7 ± 2.8	24.9 ± 4.0	0.19
Distribution of Culprit Lesions			
Right Coronary Artery	10 (22.2)	10 (37.0)	0.38
Left Descending Artery	21 (46.6)	11 (40.7)	
Left Circumflex Artery	14 (31.1)	6 (22.2)	
Number of Diseased Vessel			
1 Vessel	23 (51.1)	11 (40.7)	0.42
2 Vessels	17 (37.7)	10 (37.7)	
3 Vessels	5 (11.1)	6 (22.2)	

Values are n (%) or the mean ± SD.

Table 3 Angiographic Morphology of the Plaque Disruption Site

	Acute Myocardial Infarction n=32	Unstable Angina n=23	P
IIa	28	15	0.11
IIc	0	1	
IId	4	7	

Values are n (%) or the mean ± SD.

Table 4 Differentiation of the Plaque Disruption Site in patients with MI

	ST elevation MI n=34	Non-ST elevation MI n=11	P
Upstream	21	6	0.73
Downstream	13	5	

Values are n (%). MI indicates myocardial infarction

disruption of the upstream part and that UA arises from a plaque disruption of the downstream part in most cases. A disruption of the vulnerable plaque exposes the thrombogenic contents of an atheroma to flowing coronary blood and initiates thrombus formation, which may lead to either a blood-flow limitation or total occlusion[3,7]. The degree of flow interruption is influenced by several factors, such as the magnitude of plaque rupture, the severity of pre-existing coronary stenosis, the amount of thrombus adhering to the plaque rupture site, the lability of the thrombus, the balance of coagulability, and the severity of coronary spasm. All these factors may influence on the clinical setting of AMI and UA.

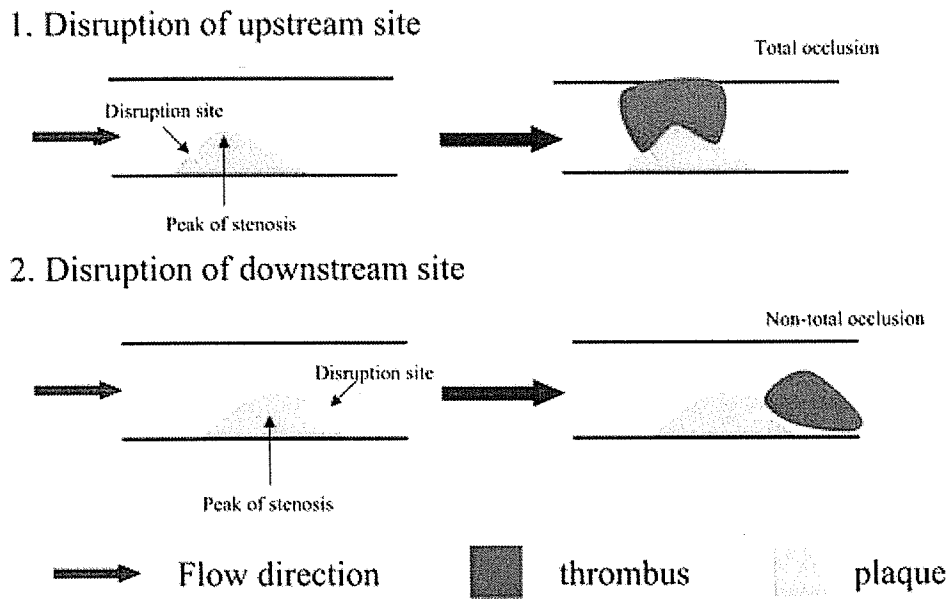

Fig. 4 Relation between the Plaque Disruption Site and Flow Interruption

Previous Mechanisms to Differentiate AMI and UA

A disruption of the atheromatous plaque following thrombus formation is believed to be the initial step in the onset of ACS. Fuster et al. have proposed the following explanation for differences between AMI and UA[3,8]. In UA with progressive symptoms, but without chest pain at rest, a plaque rupture with a change in the geometric configuration of the plaque, but without any overlying thrombus, can increase the severity of pre-existing stenosis. However, in the case of UA with chest pain at rest, the plaque rupture and pre-existing stenosis are both less severe, and, therefore, thrombosis is transient or labile. An incomplete interruption of blood flow leads to UA. In AMI, the plaque disruption is deeper than in UA, and the thrombus, which is anchored to a large rupture site, is more firmly fixed. The duration of coronary artery occlusion in AMI is also longer than in UA[9].

In terms of an interruption of blood flow, our previous angioscopic study revealed occluded red thrombi, which are formed by blood stasis, in patients with AMI. On the other hand, nonoccluded white thrombi, which are formed through incomplete interruption of blood flow, were observed in patients with UA[10]. In addition to the severity of blood flow limitation, other mechanisms that might be used to distinguish AMI from UA are vessel wall injury and hypercoagulability[11,12].

Plaque Disruption Sites

Plaque disruption often occurs on a thin fibrous cap that is composed of abundant inflammatory cells and scant smooth muscle cells (SMCs). Recently, Dirksen et al. investigated the relationship between blood-flow direction and the cellular composition of carotid plaques in a consecutive autopsy series of 45 patients. They found that the upstream shoulder of plaques tended to contain more macrophages than did the downstream shoulder. They also found that many rupture sites were located in the upstream part of the plaque[13]. Experimental studies have shown that high shear stress increases expression of endothelial adhesion molecules, such as intercellular adhesion molecule and vascular cell adhesion molecule, thus resulting in enhanced leukocyte adherence[14,15]. The upstream shoulder is exposed to high shear stress, which activates endothelium-derived nitric oxide (NO) synthesis and NO production. This chronically enhanced NO production inhibits SMC protein synthesis and SMC proliferation[16,17]. Conversely, the downstream shoulder part of the plaque, which has a relatively

low shear stress, shows larger SMC-rich areas than does the upstream part. Since the upstream shoulder of the plaque contains many inflammatory cells and few SMCs, it is more fragile than the downstream shoulder, which contains many SMCs.

Mechanical stress might also influence the development of plaque rupture. Richardson et al. investigated plaque disruption sites in autopsy cases. In cases with extracellular lipid pools in the intima, many plaque disruptions occurred at the junction of the plaque cap and the center of the plaque cap. The differentiation of the plaque disruption site was influenced by the degree of circumferential stress and shear force in the arterial wall and by the presence of a calcified plate within the intima[5]. From the viewpoint of mechanical stress, the downstream plaque shoulders could rupture more easily owing to the effects of such stress.

If the maximum stenotic site is located distal to plaque disruption, then the part of the disrupted plaque with thrombus may cause either severe stenosis or occlusion in the artery. This condition may lead to AMI. On the other hand, if maximum stenosis site is proximal to plaque disruption, then plaque disruption followed by thrombus might not induce total occlusion (**Fig. 4**). This study thus suggests that the plaque rupture site might be an important factor for distinguishing UA and AMI.

Study Limitations

We excluded totally occluded lesions and very small arteries on angiograms, because their rupture sites were unclear. In this study, the plaque ruptures in 119 of 348 patients (34.1%) and plaque rupture sites in 72 of 348 patients (20.6%) were clearly detected by angiograms. Rioufol et al. could identify plaque ruptures in 9 of 24 (37.5%) patients with ACS using intravascular ultrasound[18]. It is difficult to identify plaque disruption sites with angiography, as with other modalities, because of superimposed thrombi. The findings of Rioufol et al. are consistent with the small percentage of patients in whom plaque rupture sites could be accurately determined in our study.

Conclusions

The frequency of upstream disruption was higher in patients with AMI, whereas the frequency of downstream disruption was higher in patients with UA. This angiographic study showed that plaque disruption site might be used to distinguish UA and AMI.

References

1. Mizuno K, Miyamoto A, Satomura K, et al.: Angioscopic coronary macromorphology in patients with acute coronary disorders. Lancet 1991; 6: 809–812.
2. Falk E, Shah PK, Fuster V: Coronary plaque disruption. Circulation 1995; 92: 657–671.
3. Fuster V, Badimon L, Badimon J, Chesebro J: The pathogenesis of coronary artery disease and acute coronary syndrome. N Eng J Med 1992; 326: 310–318.
4. Libby P: Molecular bases of the acute coronary syndrome. Circulation 1995; 91: 2844–2850.
5. Richardson PD, Davies MJ, Born GVR: Influence of plaque configuration and stress distribution on fissuring of coronary atherosclerotic plaques. Lancet 1989; 21: 941–944.
6. Nagoshi T, Koiwaya Y, Doi H, Eto T: Angiographic coronary morphology in patients with ischemic heart disease. J Cardiol 2000; 36: 91–102.
7. Daves MJ, Thomas AC: Plaque fissuring: the cause of acute myocardial infarction, sudden ischemic death, and crescendo angina. Br Heart J 1985; 53: 363–373.
8. Fuster V, Badimon L, Badimon J, Chesebro J: The pathogenesis of coronary artery disease and acute coronary syndrome. N Eng J Med 1992; 326: 242–250.
9. Zaacks SM, Liebson PR, Calvin JE, Parrillo JE, Klein LW: Unstable angina and non-Q wave myocardial infarction: Dose the Clinical Diagnosis Have Therapeutic Implications? J Am Coll Cardiol 1999; 33: 107–118.
10. Mizuno K, Satomura K, Miyamoto A, et al.: Angioscopic evaluation of coronary-artery thrombi in acute coronary syndromes. N Eng J Med 1992; 326: 287–291.
11. Gimbrone MA Jr, Cybulsky MI, Kume N, Collins T, Resnick N: Vascular endothelium: an integrator of pathophysiological stimuli in atherogenesis. Ann NY Acad Sci 1995; 748: 122–132.
12. Ambrose JA: Plaque disruption and the acute coronary syndrome of unstable angina and myocardial infarction: If the substrate is similar, why is the clinical presentation different? J Am Coll Cardiol 1992; 19: 1653–1658.
13. Dirksen MT, Van der Wal AC, Van den Berg FM, Van der Loos CM, Becker AE: Distribution of inflammatory cells atherosclerotic plaque relates to the direction of flow. Circulation 1998; 98: 2000–2003.
14. Walpola PL, Gotlieb AI, Cybulsky MI, Langille BL:

Expression of ICAM-1 and VCAM-1 and monocyte adherence in arteries exposed to altered shear stress. Arterioscler Thromb Vasc Biol 1995; 15: 2–10.
15. Tropea BI, Huie P, Cooke JP, et al.: Hypertension-enhanced monocyte adhesion in experimental atherosclerosis. J Vasc Surg 1996; 23: 596–605.
16. Kolpakov V, Gordon D, Kulik TJ: Nitric oxide-generating compounds inhibit total protein and collagen synthesis in cultured vascular smooth muscle cells. Circ Res 1995; 76: 305–309.
17. Garg UC, Hassid A: Nitric oxide-generating vasodilators and 8-bromo-cyclic GMP inhibit mitogenesis and proliferation of cultured rat vascular smooth muscle cells. J Clin Invest 1989; 83: 1774–1777.
18. Rioufol G, Finet G, Ginon I, et al.: Multiple atherosclerotic plaque rupture in acute coronary syndrome. Circulation 2002; 106: 804–808.

(Received, February 23, 2006)
(Accepted, April 10, 2006)

Stent-Based Delivery of Antisense Oligodeoxynucleotides Targeted to the PDGF A-Chain Decreases In-Stent Restenosis of the Coronary Artery

Yuxin Li, MD, PhD, Noboru Fukuda, MD,† Satoshi Kunimoto, MD,* Shin-ichiro Yokoyama, MD,* Kazuhiro Hagikura, MD,* Taro Kawano, MD,* Tadateru Takayama, MD,* Junko Honye, MD,* Naohiko Kobayashi, MD,‡ Hideo Mugishima, MD,§ Satoshi Saito, MD,* and Kazuo Serie¶*

Background: Although the use of drug-eluting stents (DESs) has been shown to limit neointima hyperplasia, currently available DESs may adversely affect reendothelialization, possibly precipitating cardiac events. We evaluated the effect of an antisense oligodeoxynucleotide (ODN) targeted to the platelet-derived growth factor (PDGF) A-chain on in-stent restenosis in pig coronary artery.

Methods: A bare metal stent coated with phosphorothioate-linked antisense ODN or nonsense ODN, or a bare metal stent without ODN (control), was implanted in the mid segment of the left anterior descending artery (LAD). Twenty-eight days after implantation, angiography and intravascular ultrasound (IVUS) were performed, the LAD was removed, and stenosis was evaluated pathologically.

Results: Volumetric stenosis ratios were 64 ± 11.9, 44 ± 3.4, and 26 ± 3.8% in coronary arteries implanted with control, nonsense ODN-coated, and antisense ODN-coated stents, respectively. In angioscopic findings, the lumen surface was smooth in the stented segments in all groups. Struts of antisense ODN-coated stents were observed embedded in the neointima, whereas embedding was not observed in nonsense ODN-coated stents or control stents, indicating a decrease in hyperplasia in response to antisense ODN treatment. Pathologic findings showed 77 ± 5.8, 68 ± 12.2, and 38 ± 5.3% stenosis in coronary arteries implanted with control stents, nonsense ODN-coated stents, and antisense ODN-coated stents, respectively. A continuous lining of endothelial cells was observed along the lumen of coronary arteries implanted with antisense ODN-coated stents.

Conclusions: Stent-based delivery of an antisense ODN targeted to the PDGF A-chain effectively inhibits neointima formation after stent implantation in pig coronary artery by suppressing VSMC hyperplasia and preserving endothelialization. Antisense-ODNs may provide a therapy for in-stent restenosis of the coronary artery.

Key Words: restenosis, antisense oligonucleotides, PDGF A-chain, endothelialization

(*J Cardiovasc Pharmacol*™ 2006;48:184–190)

INTRODUCTION

Despite the widespread use of intracoronary stents, in-stent restenosis remains a major clinical problem. Neointima formation with vascular smooth muscle cell (VSMC) hyperplasia is believed to play a critical role in in-stent restenosis.[1] Drug-eluting stents (DESs) have been shown to be effective to prevent in-stent restenosis. DESs with sirolimus or paclitaxel have been used widely to prevent in-stent restenosis in humans.[2–5] Sirolimus halts cell-cycle progression,[6] and sirolimus-coated DESs can prevent in-stent restenosis by inducing complete inhibition of VSMC hyperplasia. However, complications such as subacute thrombosis or late thrombosis have been reported in patients implanted with a sirolimus-coated DES.[7,8] Sirolimus prevents reendothelialization of the inner side of the metal stent, which may cause late thrombosis. These complications have led to the development of second-generation DESs that do not induce late thrombosis.

Platelet-derived growth factor (PDGF), a potent stimulator of VSMC proliferation, is a dimer composed of a disulfide-linked polypeptides A-chain and B-chain.[9,10] There are 3 isoforms of PDGF (AA, AB, and BB). Nilsson et al[11] showed that normal growth-arrested VSMCs do not express PDGF messenger ribonucleic acid (mRNA), whereas cultured VSMCs and VSMCs in atherosclerotic plaques express PDGF A-chain mRNA and secrete PDGF-AA protein. We have reported that spontaneously hypertensive rat–derived VSMCs, which show exaggerated proliferation and the synthetic phenotype, express increased levels of PDGF A-chain mRNA.

Antisense oligodeoxynucleotides (ODNs) have been used clinically to suppress gene expression. Antisense ODNs can be used to inhibit DNA transcription and the production of mature mRNA and to inhibit peptide synthesis. Antisense therapy is being developed for the treatment of in-stent restenosis. We have shown that an antisense ODN to the PDGF A-chain inhibits the exaggerated proliferation of VSMCs from spontaneously hypertensive rats.[12–14] In a rat model of

From the *Department of Medicine, Division of Cardiovascular Medicine, Nihon University School of Medicine, Tokyo, Japan; †Advanced Research Institute for the Sciences and Humanities, Nihon University, Tokyo, Japan; ‡Department of Hypertension and Cardiorenal Medicine, Dokkyo University School of Medicine, Tochigi, Japan; §Department of Advanced Medicine, Division of Cell Regeneration and Transplantation, Nihon University School of Medicine, Tokyo, Japan; and ¶Gentier Biosystems Incorporation, Tokyo, Japan.

Reprints: Dr Noboru Fukuda, Advanced Research Institute for the Sciences and Humanities, Nihon University, 30-1 Oyaguchi-Kamimachi Itabashi-ku, Tokyo 173-8610, Japan (e-mail: fukudan@med.nihon-u.ac.jp).

neointima formation in the carotid artery after balloon injury, we showed a 60% decrease in neointima in response to antisense therapy.

To aid in the development of safer DESs that do not inhibit reendothelialization, we examined the effects of stent-based delivery of an antisense ODN targeted to the PDGF A-chain on in-stent restenosis and reendothelialization of the coronary artery in pigs.

METHODS

Synthetic Antisense Oligodeoxynucleotides to the Platelet-Derived Growth Factor (A-chain)

We used a 15-mer antisense ODN to the PDGF A-chain (5′-AGGTCCTCATCGCGT-3′) complementary to the region containing the initiation codon of human and rat PDGF A-chain complementary deoxyribonucleic acid (cDNA), as reported previously.[12] A nonsense control ODN (5′-TGCCGTCAGCTGCTA-3′) contained an identical proportion of bases but in random order. ODNs were synthesized with a DNA synthesizer (model 394; Applied Biosystems, Foster City, CA, USA) and purified on an OPC column (Applied Biosystems). ODNs were modified with a phosphorothioate linkage by oxidizing phosphate linkages with 3H-1,2-benzodithiol-3-one-1,1-dioxide instead of the standard iodine reagent.[15]

Animal Preparation and Stent Implantation

Animal care and handling were performed in accordance with the National Institutes of Health Guide for the Care and Use of Laboratory Animals and were approved by the Institutional Animal Care and Use Committee of Nihon University. Eighteen domestic male pigs weighing 22–28 kg each were used in the present study. Bare metal stents (n = 6), nonsense ODN-coated stents (n = 3), and antisense ODN-coated stents (n = 9) were implanted into the left anterior descending artery. Hydrogel-coated matrical stents (diameter 3.5 mm, length 20 mm, Interventional Radiology Co., Ltd., Tokyo, Japan) were dip-coated in 20 μg/mL antisense or nonsense ODN solution containing 100 μ/mL polyethylenimine reagent (MBI Fermentas) for 10 min and were air-dried for 10 min. Control stents were treated identically but were not coated with ODN.[16,17]

Aspirin (325 mg) was administered 1 day before stent implantation. After overnight fasting, intramuscular injection of 25 mg/kg sodium pentobarbital was administered and anesthesia was maintained with a continuous intravenous infusion of 1mg/kg per hour ketamine chloride. A 5000-IU bolus of heparin was administered intravenously. After endotracheal intubation, controlled mechanical ventilation was established at a tidal volume of 10–15 mL/kg with a volume-cycle ventilator (Servo 900-E; Siemens-Elema Inc, Stockholm, Sweden).

Continuous hemodynamic and surface electrocardiography monitoring were maintained throughout the procedure. The right carotid artery was inserted with a 6F sheath. After baseline coronary angiography, mechanical intravascular ultrasound (IVUS) (40 MHz, Atlantis™; Boston Scientific Corp., Natick, MA, USA) of the left anterior descending artery was performed. IVUS catheters were automatically pulled back at 0.5 mm per second. IVUS images were recorded continuously on Super VHS videotape for analysis. Based on the IVUS images, a segment of diameter of 3.0 mm in diameter was selected for stent implantation. Stents of 3.5 mm × 20 mm were used with a 12-atm inflation pressure to reach a 1.3:1 stent-to-artery ratio. Immediately after implantation, IVUS was performed to confirm the stent-to-artery ratio. If the ratio was not adequate, the stent balloon was reinflated with higher pressure in the stented segment. Follow-up coronary angiography and IVUS were performed 28 days after implantation, and the stented coronary arteries were harvested for angioscopic evaluation and pathologic analysis.

To assess the distribution of antisense ODN targeted to the PDGF A-chain, stents coated with fluorescein-isothiocyanate (FITC)-labeled antisense ODN were implanted. Twenty-four hours after implantation, the heart was removed, and the stented coronary artery segment was harvested and fixed in 4% paraformaldehyde. Sections were examined by fluorescence microscopy. In addition, 3.5 mm × 23 mm sirolimus-coated stents (Cypher™; Cordis Corp., Miami Lakes, FL, USA) were implanted by the same method. After 28 days, the stented coronary artery segment was harvested for angioscopic evaluation and pathologic analysis.

Intravascular Ultrasound Measurements

Follow-up IVUS images were recorded on Super VHS tape and analyzed with a computer-based contour detection program for 3-dimensional reconstruction and volumetric measurement (NetraIVUS™ software package for Windows NT®, ScImage Corp, Los Altos, CA, USA). Cross grids recorded on the IVUS images were used for calibration. The interface between the neointima and lumen and the outer border of the external elastic membrane were traced manually. On the basis of the manual traces, the computer software determined measurements for lumen volume (LV) and vessel volume (VV). Volumetric in-stent restenosis (%AS) was calculated as (VV-LV)/VV.

Angioscopic Evaluations

Twenty-eight days after stent implantation, the stented segment of coronary artery was harvested after perfusion with saline at physiologic pressure. Angioscopic observations were made while the blood was perfused away. We used an MC-800E angioscope (Nihon Kohden, Tokyo, Japan) and an AS-003 optic fiber (Nihon Kohden). We examined the entire stented segment from the distal to the proximal end and evaluated the inner surface for neointima and thrombi.

Pathologic Analysis

Three cross sections were cut for pathologic analysis, 1 each from the proximal, central, and distal portions along each stent. Sections were ground to a thickness of approximately 50 μm and stained with hematoxylin and eosin. A computerized imaging system (ImageJ 1.30, NIH) was used for histomorphometric measurements of the following parameters: lumen area, defined as the area circumscribed by the neointima–lumen border, and neointima area, defined as the area between the lumen and the internal elastic lamina (IEL). In-stent restenosis was estimated as the neointima area/IEL area.

Statistical Analysis

Data are expressed as mean ± SEM. Mean values of variables were compared by a 2-sided unpaired *t*-test. A value of $P < 0.05$ was considered statistically significant.

RESULTS

Distribution of Antisense Oligodeoxynucleotide Targeted to the PDGF A-Chain

The distribution of FITC-labeled antisense ODN 24 hours after implantation is shown in Figure 1. FITC-labeled antisense ODN was distributed predominantly in the endothelial layer of the stented coronary artery.

IVUS Findings of In-Stent Restenosis

The stent/artery ratio was 1.3 ± 0.1, 1.3 ± 0.1, and 1.4 ± 0.1 in coronary arteries implanted with bare metal stents, nonsense ODN-coated stents, and antisense ODN-coated stents, respectively. There were no significant differences between the 3 groups.

Occlusive neointima filled the lumen and encircled the ultrasound catheter in arteries implanted with control stents (Fig. 2A, B), whereas the lumen was clear in coronary arteries implanted with antisense ODN-coated stents (Fig. 2C, D). Volumetric in-stent restenosis ratios were 64 ± 11.9, 44 ± 3.4, and 26 ± 3.8% in coronary arteries implanted with bare metal stents, nonsense ODN-coated stents, and antisense ODN-coated stents, respectively. The in-stent restenosis ratio was significantly less in the antisense group than in the control and nonsense groups (Fig. 2E).

Angioscopic Findings

The lumen surface was smooth and lacked protrusions in the stented segments of coronary arteries in all groups (Fig. 3A–C). Struts in the antisense ODN-coated stent group were visibly embedded in the neointima (Fig. 3C), whereas embedding was invisible in the nonsense ODN-coated stent and control stent groups, indicating decreased neointimal hyperplasia in the antisense group. An irregular surface with protrusions into the lumen were observed in sirolimus-coated stented segments, and some ragged red thrombi were observed adhering to the lumen surface (Fig. 3D).

Pathologic Findings

Microscopic images obtained 28 days after implantations are shown in Figure 4. Neointima formation was less in coronary arteries implanted with antisense ODN-coated stents than in arteries implanted with control stents or nonsense ODN-coated stents. In-stent stenosis in distal, central, and proximal areas of stented artery are shown in Figure 5. In-stent stenosis of control, antisense, and nonsense groups was 70 ± 9.7, 58 ± 4.2, and 41 ± 5.5% in the proximal end; 77 ± 5.8, 68 ± 12.2, and 38 ± 5.3% in the central segment; and 65 ± 9.1, 70 ± 4.9, and 38 ± 5.9% in the distal end. These findings indicate that the antisense ODN targeted to the PDGF A-chain significantly inhibited in-stent neointima formation.

Differences in endothelialization differed between sirolimus-coated stents and antisense ODN-coated stents (Fig. 6). Patchy and interrupted endothelial cells in the artery lumen were observed in arteries implanted with sirolimus-coated stents (Fig. 6A), whereas a continuous lining of endothelial cells was observed in arteries implanted with antisense ODN-coated stents (Fig. 6B). There is no difference in appearance of reendothelialization among antisense ODN-coated stent, nonsense ODN-coated stent, and bare metal stent. These data suggest that the antisense ODN does not interfere with in-stent endothelialization.

DISCUSSION

Various classes of agents are available and are under investigation for the use of DESs to prevent in-stent restenosis of the coronary artery and include immunosuppressive (sirolimus), antiinflammatory (corticoid and tranilast), antiproliferative (paclitaxel, angiopeptin, and actinomycin), and antithrombotic agents (hirudin and iloprost).[18] Sirolimus halts cell-cycle progression at the G1 phase, resulting in inhibition of replication and proliferation.[6] Sirolimus halts the cell cycle nonspecifically; therefore, sirolimus-coated DESs prevent not only VSMC hyperplasia but also endothelialization, which is required for the prevention of thrombosis. Patients implanted with a sirolimus-coated DES require the administration of antiplatelet agents for at least 3 months after stent implantation.

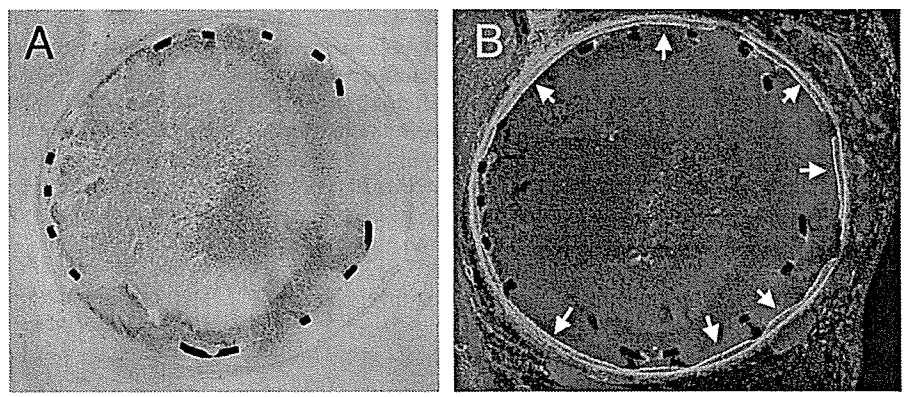

FIGURE 1. Distribution of FITC-labeled antisense ODN targeted to the PDGF A-chain in a stent 24 hours after implantation in a pig coronary artery. A. Optical microscopy. B, Fluorescence microscopy. Arrows in (B) indicate areas of ODN fluorescence.

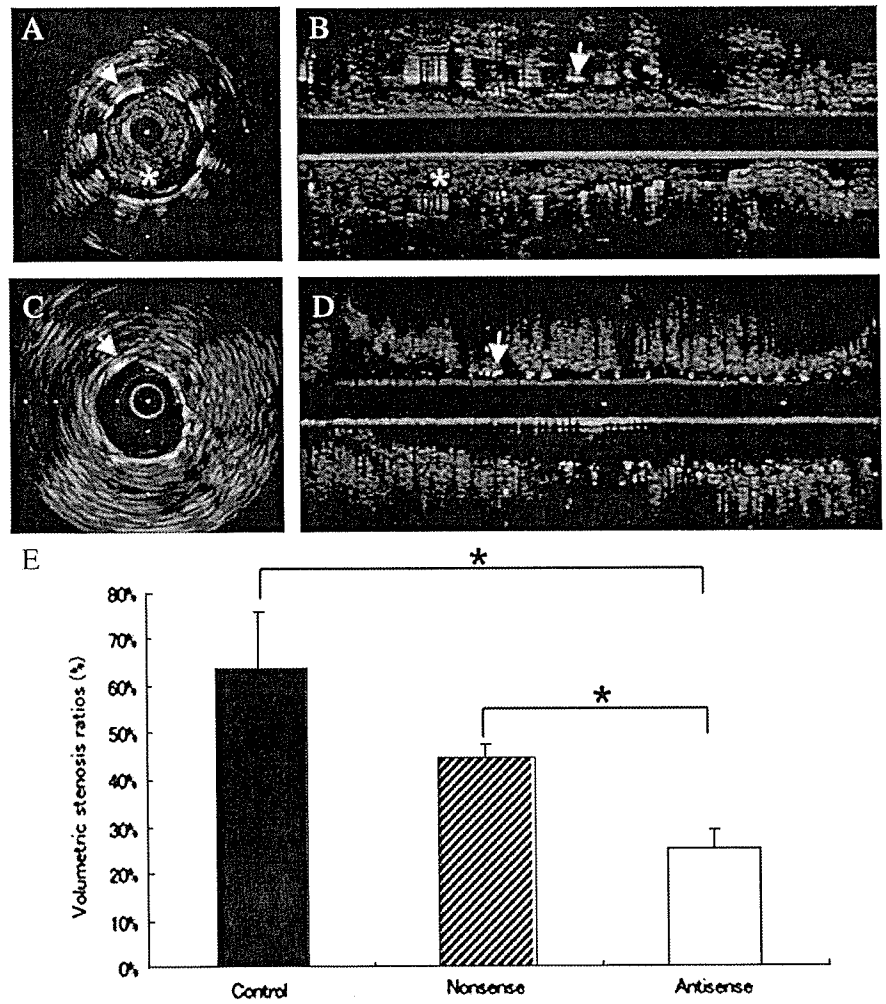

FIGURE 2. Representative cross sections (A, C) and long-axis images (B, D) of coronary arteries implanted with bare metal stents (A, B) or with antisense ODN-coated stents (C, D) assessed by intravascular ultrasound 28 days after implantation. Arrows indicate stent struts. Stars indicate neointima. E, Volumetric stenosis ratios for antisense-coated, nonsense-coated, and control stents. Data are the mean ± SEM. $*P < 0.05$.

The timing of reendothelialization differs between patients, and late thrombosis is a major problem in patients implanted with sirolimus-coated DESs. Thus, development of DESs that preserve endothelialization is necessary.

In the present study, stent-based delivery of an antisense ODN targeted to the PDGF A-chain showed a potent inhibitory effect on VSMC proliferation, showing a 60% decrease in percent volume stenosis and preservation of endothelialization. DESs with sirolimus did not preserve endothelialization.

In 2001 it was that VSMCs in the neointima originate from circulating bone marrow cells in addition to media VSMCs.[19] Intimal VSMCs, which show the synthetic phenotype, abundantly express several cytokines and growth factors, including PDGF, transforming growth factor-beta, basic fibroblast growth factor, endothelin, and angiotensin II, which are involved in neointima formation.[20] Neointima are composed of VSMCs and extracellular matrix.[21] It is likely that antisense ODN targeted to the PDGF A-chain inhibits neointima formation at least in part.

The PDGF A-chain contributes to VSMC proliferation in arterial proliferative disease. The PDGF B-chain is expressed constitutively in the vasculature and in platelets, whereas the PDGF A-chain is produced only in VSMCs of the synthetic phenotype. Kruppel-like zinc-finger transcription factor 5 (KLF5) has been established as a transcription factor that alters VSMCs from the contractile to the synthetic phenotype, inducing expression of the PDGF A-chain.[22] These findings suggest that the PDGF A-chain is a critical target for the inhibition of VSMC hyperplasia in neointima. Our results suggest that the antisense ODN targeted to the PDGF A-chain is a specific inhibitor of neointimal VSMC proliferation that does not affect endothelialization. Stent-based delivery of this antisense ODN inhibited neointima formation and preserved endothelialization in the absence of antiplatelet agents.

One problem of exogenously administered nucleic acid–based medicines, including antisense DNA, is that they are readily degraded by nucleases in vivo. However, locally delivered nucleic acids from a DES show less degradation than do systemically administered nuclei acids. In the present experiments, we chemically modified antisense ODN to the phosphorothioate type, dissolved it in hydrogel, and applied it to both the balloon and the stent, resulting in efficient delivery of

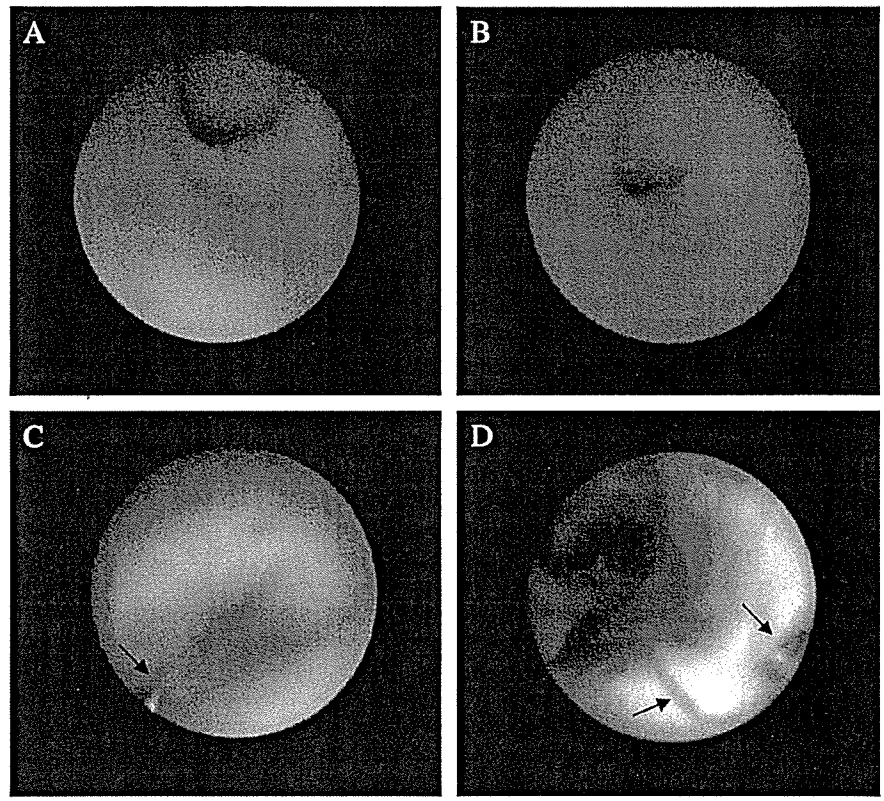

FIGURE 3. Representative angioscopic findings of stented segments of pig coronary artery implanted with bare metal stents (A), nonsense ODN-coated stents (B), antisense ODN-coated stents (C), or sirolimus-coated stents (D). Arrows indicate embedding in the neointima.

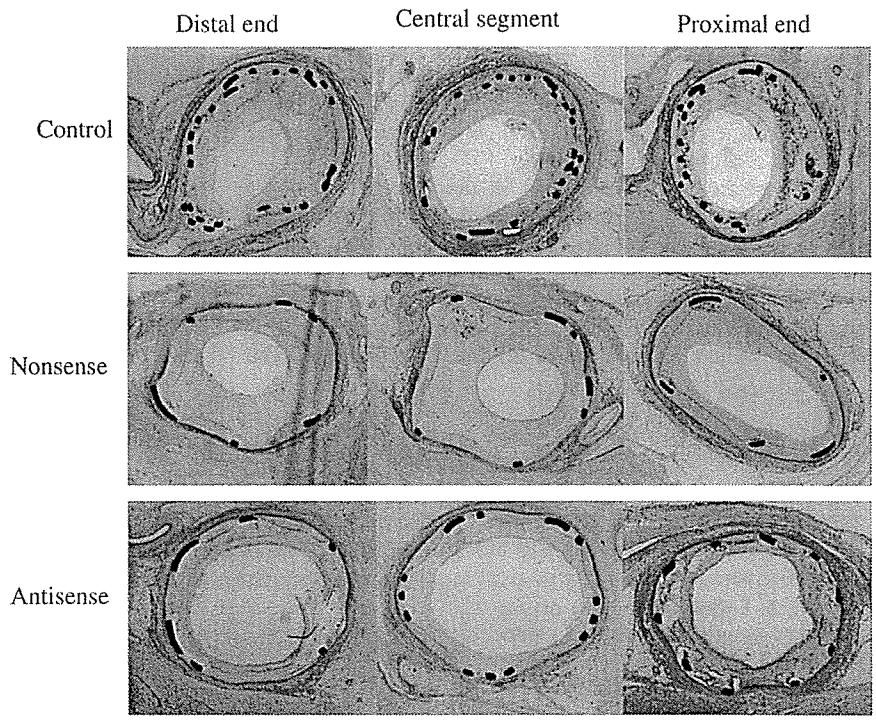

FIGURE 4. Microscopic images of pig coronary arteries implanted with bare metal stents (control), nonsense ODN-coated stents, or antisense ODN-coated stents 28 days after implantation. Sections were stained with hematoxylin and eosin.

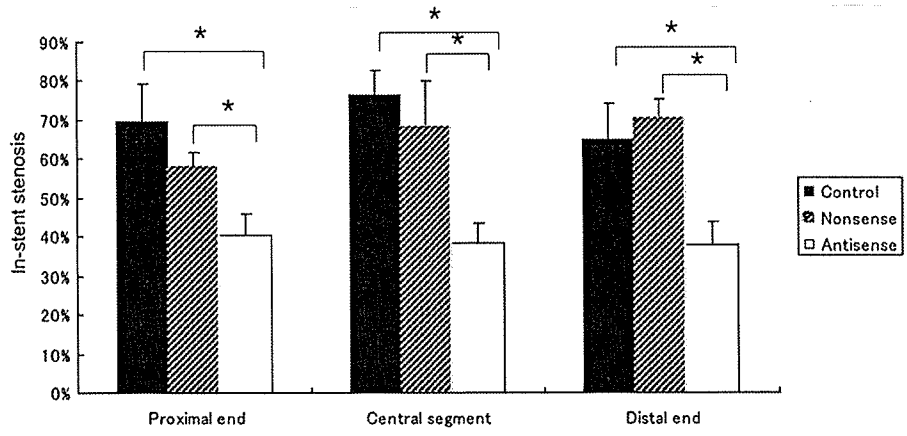

FIGURE 5. Quantification of in-stent stenosis from the microscopic images of pig coronary arteries implanted with bare metal stents (control), nonsense ODN-coated stents, or antisense ODN-coated stents 28 days after implantation. A computerized imaging system (ImageJ 1.30) was used for histomorphometric measurement of the following parameters: lumen area, defined as the area circumscribed by the neointima-lumen border, and the neointima area, defined as the area between the lumen and the internal elastic lamina (IEL). Percent in-stent restenosis was calculated as neointima area/IEL area. Data are mean ± SEM. $*P < 0.05$.

antisense ODN to the coronary artery. Nonsense ODN with a random sequence also showed a tendency to inhibit the neointima formation to a lesser extent. Similar nonspecific effects of ODN have confounded the interpretation of previous antisense studies. Several studies report that charged ODN behaves like polyanions such as heparin and heparan, which bind and sequester heparin-binding growth factors, such as basic fibroblast growth factor or PDGF, at the basement membrane.[23] Another report described the nonspecific cellular activation of the transcription factor Sp1 by phosphorothioate-linked ODN.[24]

Recent applications of antisense ODN targeted to c-myc have been reported for the prevention of in-stent stenosis of the coronary artery in pigs[25] and humans.[26] An advanced antisense ODN (AVI-4126) to c-myc–eluting stent inhibited c-myc expression and significantly inhibited neointimal hyperplasia by 40% in a pig model. C-myc is also required in the progression of cell cycle. Therefore, a DES with antisense ODN targeted to c-myc may inhibit reendothelialization in a manner similar to a sirolimus-coated DES.

There are some limitations in the present study. An important point in this animal model is that the arteries are devoid of atherosclerotic lesions, whereas in patients, most stent struts are in contact with atheromatous plaque and not with the media. In the present study, degree of in-stent restenosis was examined only at 1 month after stent implantation; longer follow-up should be performed in future experiments. The coating system in the present study is hydrogel, which is different with sirolimus-coated stents (Cypher stent). The impaired reendothelialization with the Cypher stent might be mainly related to the polymer-coated stent surface and not to the drug.[27]

Based on the results in the present study, we plan to repeat the experiments with longer follow-up and repeat the experiments in an animal model of coronary atherosclerosis. After animal experiments, we plan to apply stents coated with antisense ODN targeted to the PDGF A-chain for treatment of human coronary diseases. Clinical trials of antisense therapies have been performed for human diseases including cancer.[28,29] Even high doses of infused antisense ODN for long periods show little or no side effects or toxicity in clinical trials, indicating the safety of antisense therapy in humans. Although antisense ODNs can be applied to DESs, certain technical problems need to be addressed. In the present study, we used polyethylenimine as the delivery regent. Procedures providing more effective and safer delivery of antisense ODN from DESs should be assessed.

In the present study, we applied hydrogel to the balloon and the stent. This was particularly helpful for coating the stent with antisense ODN. We are developing a coated stent that more effectively absorbs and delivers agents to the coronary artery. At physiologic pH, antisense ODNs are negatively charged. Thus, the metal surface of the stent can be coated with a positively charged substance, enabling antisense ODNs to adhere strongly to the stent.

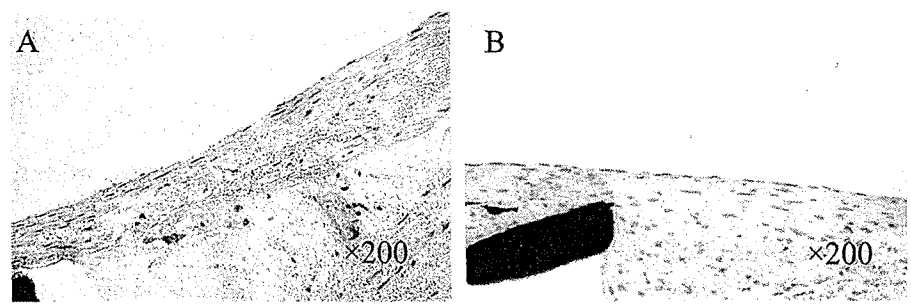

FIGURE 6. Endothelialization of pig coronary arteries implanted with antisense ODN-coated stents (A) or sirolimus-coated stents (B). Sections were stained with hematoxylin.

CONCLUSION

In conclusion, we showed that stents coated with an antisense ODN targeted to the PDGF A-chain effectively inhibited in-stent stenosis and preserved reendothelialization. These results indicate that stent-based delivery of antisense ODN targeted to the PDGF A-chain is a safe and feasible therapy for coronary arterial disease.

ACKNOWLEDGMENT

We gratefully acknowledge the expert technical assistance of Yoshiki Taniguchi.

REFERENCES

1. Virmani R, Farb A. Pathology of in-stent restenosis. *Curr Opin Lipidol.* 1999;10:499–506.
2. Cohen DJ, Bakhai A, Shi C, et al. Cost-effectiveness of sirolimus-eluting stents for treatment of complex coronary stenoses: results from the Sirolimus-Eluting Balloon Expandable Stent in the Treatment of Patients With De Novo Native Coronary Artery Lesions (SIRIUS) trial. *Circulation.* 2004;110:508–514.
3. Regar E, Serruys PW, Bode C, et al. Angiographic findings of the multicenter Randomized Study With the Sirolimus-Eluting Bx Velocity Balloon-Expandable Stent (RAVEL): sirolimus-eluting stents inhibit restenosis irrespective of the vessel size. *Circulation.* 2002;106:1949–1956.
4. Colombo A, Drzewiecki J, Banning A, et al. Randomized study to assess the effectiveness of slow- and moderate-release polymer-based paclitaxel-eluting stents for coronary artery lesions. *Circulation.* 2003;108:788–794.
5. Park SJ, Shim WH, Ho DS, et al. A paclitaxel-eluting stent for the prevention of coronary restenosis. *N Engl J Med.* 2003;348:1537–1545.
6. Murakami M, Ichisaka T, Maeda M, et al. mTOR is essential for growth and proliferation in early mouse embryos and embryonic stem cells. *Mol Cell Biol.* 2004;24:6710–6718.
7. Iakovou I, Sangiorgi GM, Stankovic G, et al. Effectiveness of sirolimus-eluting stent implantation for treatment of in-stent restenosis after brachytherapy failure. *Am J Cardiol.* 2004;94:351–354.
8. Werner GS, Emig U, Krack A, et al. Sirolimus-eluting stents for the prevention of restenosis in a worst-case scenario of diffuse and recurrent in-stent restenosis. *Cath Cardiovasc Interv.* 2004;63:259–264.
9. Hart CE, Forstrom JW, Kelly JD, et al. Two classes of PDGF receptor recognize different isoforms of PDGF. *Science.* 1988;240:1529–1531.
10. Johnsson A, Heldin CH, Westermark B, et al. Platelet-derived growth factor: identification of constituent polypeptide chains. *Biochem Biophys Res Commun.* 1982;104:66–74.
11. Nilsson J, Sjolund M, Palmberg L, et al. Arterial smooth muscle cells in primary culture produce a platelet-derived growth factor-like protein. *Proc Natl Acad Sci U S A.* 1985;82:4418–4422.
12. Fukuda N, Kubo A, Watanabe Y, et al. Antisense oligodeoxynucleotide complementary to platelet-derived growth factor A-chain messenger RNA inhibits the arterial proliferation in spontaneously hypertensive rats without altering their blood pressures. *J Hypertens.* 1997;15:1123–1136.
13. Kishioka H, Fukuda N, Nakayama M, et al. Effect of methylene methylimino linkage of antisense oligonucleotide to the platelet-derived growth factor A-chain on growth of vascular smooth muscle cells from spontaneously hypertensive rats. *Eur J Pharmacol.* 2000;392:129–132.
14. Kishioka H, Fukuda N, Wen-Yang H, et al. Effects of PDGF A-chain antisense oligodeoxynucleotides on growth of cardiovascular organs in stroke-prone spontaneously hypertensive rats. *Am J Hypertens.* 2001;14:439–445.
15. Iyer RP, Phillips LR, Egan W, et al. The automated synthesis of sulfur-containing oligodeoxyribonucleotides using 3H-1,2-benzodithiol-3-one 1,1-dioxide as a sulfur-transfer reagent. *J Org Chem.* 1990;55:4693–4699.
16. Boussif O, Lezoualc'h F, Zanta MA, et al. A versatile vector for gene and oligonucleotide transfer into cells in culture and in vivo: polyethylenimine. *Proc Natl Acad Sci U S A.* 1995;92:7297–7301.
17. Jaschke B, Michaelis C, Milz S, et al. Local statin therapy differentially interferes with smooth muscle and endothelial cell proliferation and reduces neointima on a drug-eluting stent platform. *Cardiovasc Res.* 2005;68:483–492.
18. Wong A, Chan C. Drug-eluting stents: the end of restenosis? *Ann Acad Med Singapore.* 2004;33:423–431.
19. Han CI, Campbell GR, Campbell JH. Circulating bone marrow cells can contribute to neointimal formation. *J Vasc Res.* 2001;38:113–119.
20. Carmeliet P, Moons L, Dewerchin M, et al. Insights in vessel development and vascular disorders using targeted inactivation and transfer of vascular endothelial growth factor, the tissue factor receptor, and the plasminogen system. *Ann N Y Acad Sci.* 1997;811:191–206.
21. Majesky MW. Neointima formation after acute vascular injury. Role of counteradhesive extracellular matrix proteins. *Tex Heart Inst J.* 1994;21:78–85.
22. Shindo T, Manabe I, Fukushima Y, et al. Kruppel-like zinc-finger transcription factor KLF5/BTEB2 is a target for angiotensin II signaling and an essential regulator of cardiovascular remodeling. *Nat Med.* 2002;8:856–863.
23. Wellstein A, Zugmaier G, Califano JA 3rd, et al. Tumor growth dependent on Kaposi's sarcoma-derived fibroblast growth factor inhibited by pentosan polysulfate. *J Natl Cancer Inst.* 1991;83:716–720.
24. Perez JR, Li Y, Stein CA, et al. Sequence-independent induction of Sp1 transcription factor activity by phosphorothioate oligodeoxynucleotides. *Proc Natl Acad Sci U S A.* 1994;91:5957–5961.
25. Kipshidze NN, Iversen P, Kim HS, et al. Advanced c-myc antisense (AVI-4126)-eluting phosphorylcholine-coated stent implantation is associated with complete vascular healing and reduced neointimal formation in the porcine coronary restenosis model. *Cath Cardiovasc Interv.* 2004;61:518–527.
26. Kutryk MJ, Foley DP, van den Brand M, et al. Local intracoronary administration of antisense oligonucleotide against c-myc for the prevention of in-stent restenosis: results of the randomized investigation by the Thoraxcenter of antisense DNA using local delivery and IVUS after coronary stenting (ITALICS) trial. *J Am Coll Cardiol.* 2002;39:281–287.
27. Hausleiter J, Kastrati A, Wessely R, et al. Prevention of restenosis by a novel drug-eluting stent system with a dose-adjustable, polymer-free, on-site stent coating. *Eur Heart J.* 2005;26:1475–1481.
28. Advani R, Peethambaram P, Lum BL, et al. A Phase II trial of aprinocarsen, an antisense oligonucleotide inhibitor of protein kinase C alpha, administered as a 21-day infusion to patients with advanced ovarian carcinoma. *Cancer.* 2004;100:321–326.
29. Marshall J, Chen H, Yang D, et al. A phase I trial of a Bcl-2 antisense (G3139) and weekly docetaxel in patients with advanced breast cancer and other solid tumors. *Ann Oncol.* 2004;15:1274–1283.

ELSEVIER
International Journal of Cardiology xx (2006) xxx–xxx
International Journal of Cardiology
www.elsevier.com/locate/ijcard

Letter to the Editor

Generalized spasm of the right coronary artery after successful stent implantation provoked by intracoronary administration of ergonovine

Yuxin Li, Junko Honye *, Tadateru Takayama, Satoshi Saito

Division of Cardiovascular Medicine, Department of Medicine, Nihon University School of Medicine, 30-1, Oyaguchi-Kami-machi, Itabashi-ku, Tokyo 173-8610, Japan

Received 1 March 2006; received in revised form 23 July 2006; accepted 29 July 2006

Abstract

Coronary spasm may be one of the reasons for the appearance of chest pain after successful percutaneous coronary interventions, and is potentially hazardous when myocardial ischemia occurs. Coronary spasm can be diagnosed by intracoronary administration of ergonovine as a selective spasm provocative test. We report here the case of a patient who had chest pain and ST segment elevation 10 days after successful right coronary artery stent implantation. Repeat angiography was performed, with results of no in-stent stenosis and no stenosis in other segments. Since coronary artery spasm was considered as a possible reason, a spasm provocative test was attempted. Following ergonovine administration (total dose, 50 μg) into the right coronary artery, severe spasm with 99% stenosis developed over the whole artery except the stented segment. Isosorbide dinitrate was injected immediately, and the provoked spasm was soon relieved. Intravascular ultrasound revealed no neointima at the stented segment and diffuse and mild low-echogenic concentric plaque at the distal as well as proximal segment of the stent. Most reports regarding coronary artery spasm provocative tests have focused on focal lesions before interventional therapy, or during interventional procedures. Although it is quite rare, potential coronary spasm should be considered when chest symptoms recur after percutaneous coronary interventions without angiographic representation.

Keywords: Coronary artery generalized spasm; Provocative test; Percutaneous coronary interventions; Intravascular ultrasound

1. Introduction

Coronary artery spasm is an important component in the clinical spectrum of coronary artery disease and is thought to represent the main pathogenetic mechanism of variant angina. There have been several studies on coronary artery spasm; however, most of them focused on focal spasm and lesions before interventional therapy [1–4]. Although coronary artery spasm after successful interventional therapy has rarely been reported, it may cause recurrent chest pain and ischemia even after coronary interventions. Coronary artery spasm can be diagnosed by provocative tests, using intravenous or intracoronary administration of ergonovine [1,5,6]. We report here a patient who developed generalized spasm of the right coronary artery after successful stent implantation, which was provoked by intracoronary administration of ergonovine.

2. Case report

A 57-year-old man presenting with severe chest pain, diagnosed as AMI at another clinic, was referred to our coronary care unit. He developed 2nd degree AV block and marked ST segment elevation in leads II, III, and aVF. Emergency coronary angiography revealed total occlusion of the proximal right coronary artery. Successful stent implantation was performed on the culprit lesion without residual stenosis. The patient was transferred to the general cardiovascular ward after the interventional therapy. However, 10 days later, he experienced recurrent chest pain at 9:30 pm

* Corresponding author. Tel.: +81 3 3972 8111x2413; fax: +81 3 3972 1098.
E-mail address: hone-circ@umin.ac.jp (J. Honye).

0167-5273/$ - see front matter © 2006 Elsevier Ireland Ltd. All rights reserved.
doi:10.1016/j.ijcard.2006.07.137

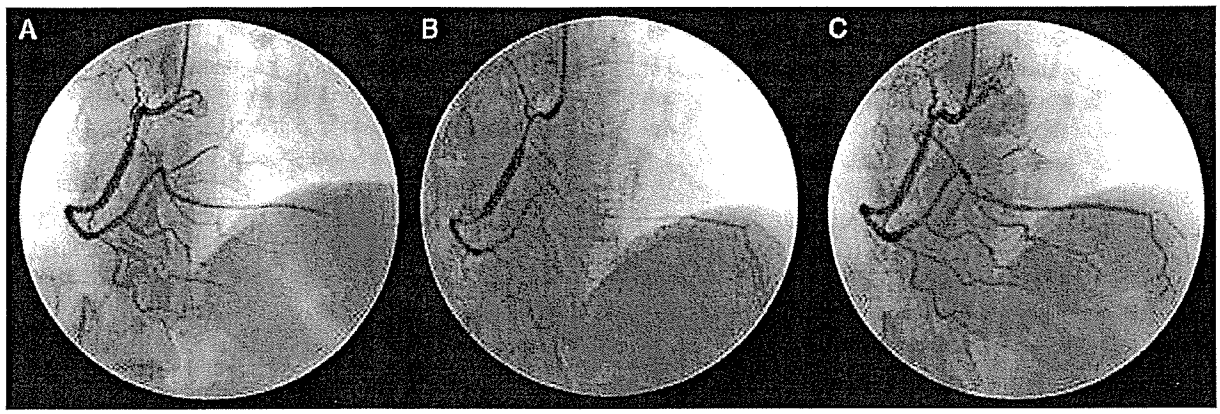

Fig. 1. A: Baseline coronary angiogram of the right coronary artery showing no in-stent restenosis and stenosis in other segments. B: Following intracoronary administration of ergonovine, diffuse spasm was provoked over the whole right coronary artery except the stented segment. C: After intracoronary administration of isosorbide dinitrate, the provoked spasm was relieved.

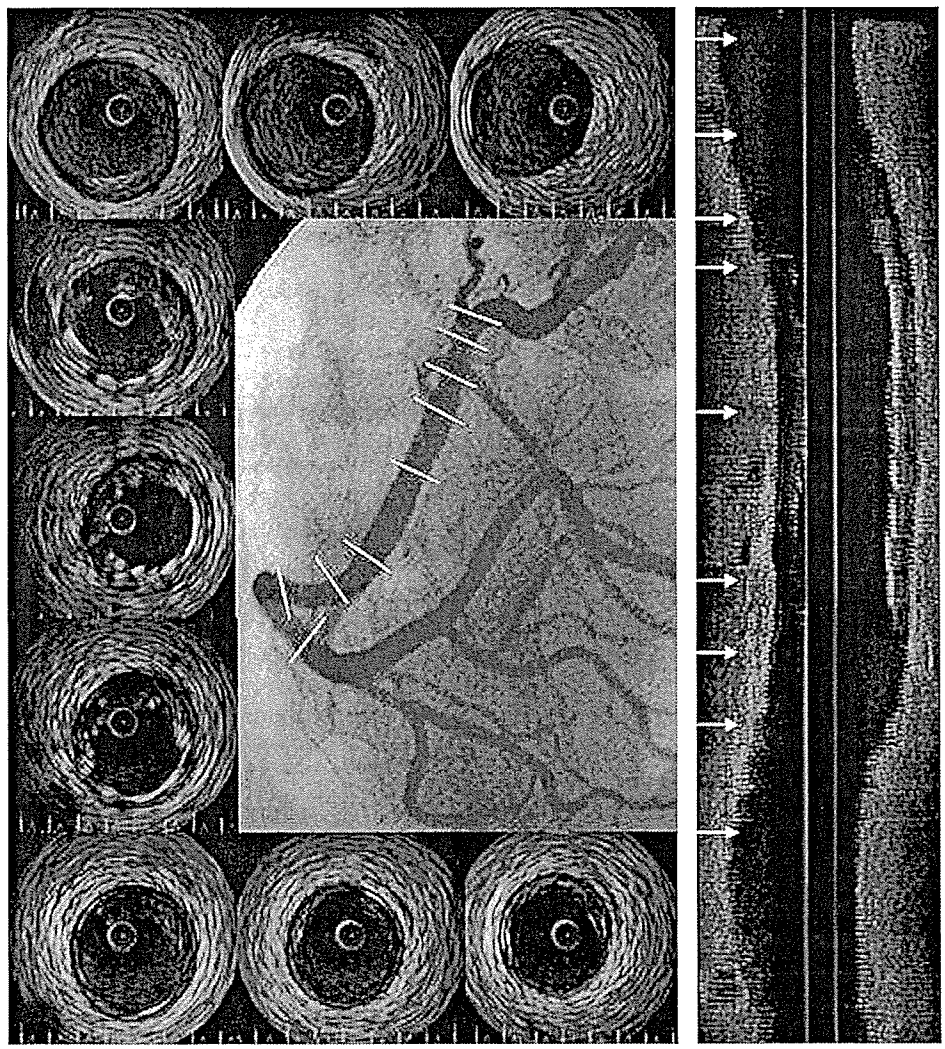

Fig. 2. Angiogram and IVUS images of the right coronary artery. Cross sectional images of the IVUS are shown on the left, and a longitudinal section image is shown on the right. In the stented segment, there is no neointima within the stent. In the distal as well as proximal segment of the stent, diffuse non-calcified mild concentric low-echogenic plaque can be seen on the IVUS images.

Please cite this article as: Yuxin Li et al., Generalized spasm of the right coronary artery after successful stent implantation provoked by intracoronary administration of ergonovine, International Journal of Cardiology (2006), doi:10.1016/j.ijcard.2006.07.137

and 4:30 am with ST segment elevation on Holter ECG. He underwent a repeat angiogram because of the recurrent angina with electrocardiographic changes. The angiogram did not demonstrate in-stent stenosis or other coronary stenosis (Fig. 1A). Coronary artery spasm was considered a strong possibility because of these symptoms and the electrocardiographic changes, and an ergonovine provocative test was therefore attempted after routine coronary angiography. An initial dose of 10 μg ergonovine maleate solution was injected into the right coronary artery and subsequent injections of 20 μg were repeated every 3 min, until evident spasm occurred or the total dose of ergonovine reached 50 μg [2]. Following administration of ergonovine with a total dose of 50 μg, the patient complained of chest pain and coronary angiography demonstrated severe spasm with 99% stenosis over the whole right coronary artery except the stented segment (Fig. 1B). Immediately after, 2.5 mg isosorbide dinitrate was injected into the right coronary artery; the spasm was relieved and the symptoms also disappeared (Fig. 1C). The left coronary artery did not develop spasm after the ergonovine provocative test on the right coronary artery. Intravascular ultrasound (IVUS) of the right coronary artery was performed with auto-pullback at 0.5 mm/s. In the stented segment, there was no neointima within the stent. At the distal as well as proximal segment of the stent, diffuse mild concentric low echogenic plaque without calcification was observed (Fig. 2). Based on these findings, nitrate and calcium antagonists were administered. There was no recurrence of symptoms during follow-up. An exercise tolerance test and myocardial perfusion scintigraphy did not reveal ischemia. Repeat coronary angiography at 6 months follow-up failed to demonstrate restenosis at the stented segment and stenosis at other segments of the right coronary artery and left coronary artery.

3. Discussion

Chest pain after successful percutaneous coronary intervention constitutes a notable problem and may be potentially life threatening when myocardial ischemia occurs. Such pain suggests the presence of residual coronary stenosis, acute closure, coronary spasm or myocardial infarction. Management of each type of patient includes repeat coronary angiography and additional intervention. Coronary artery stenosis or acute closure can be clearly revealed by coronary angiography, whereas coronary spasm is difficult to demonstrate by routine angiography. Prolonged spasm is very dangerous, it might cause plaque rupture or/and prolonged coronary flow limitation and induce acute thrombus [3]. Coronary artery spasm can be diagnosed by the intracoronary administration of ergonovine as a selective provocative test [1,2,5,6].

Coronary artery spasm after stent implantation has rarely been reported. In the present case, although Holter ECG with chest pain revealed significant ischemic changes, coronary angiography did not show stenosis. Coronary artery spasm was considered to be the reason for the ischemic attack, and the ergonovine provocative test confirmed coronary artery spasm except in the stented segment. Previous researches have indicated that the frequency of coronary spasm is higher in Japanese than in Caucasians [1].

In a previous IVUS study, we found that coronary spasm is associated with the presence of moderate atherosclerosis without calcification [2]. In the present case, although there was no angiographic stenosis at the segment with spasm, IVUS demonstrated mild atherosclerotic plaque. This finding agrees with our previous IVUS results and other histological studies [2]. From our experience, non-calcified moderate eccentric plaque appears to be closely related to focal spasm, while generalized spasm as in the present case is associated with mild and diffuse concentric plaque. In the clinical setting, coronary spasm is most common in patients aged at around 50 years, and it decreases as age advances [7]. With older patients, coronary artery plaque calcification may reflect this situation. Some studies have shown that during the development of atherosclerosis, chemical mediators such as cytokines could be possible messengers for the induction of coronary spasm. Depressed production of nitric oxide appears to be another mechanism of spasm in the presence of atherosclerotic lesions [8]. Since non-calcified moderate atherosclerotic plaque seems to be closely related to the occurrence of coronary spasm, occult atherosclerotic lesions with documented vasospasm should be treated with nitrate and calcium antagonist. In about 5–30% patients, high doses of calcium antagonists and nitrates are not effective for the treatment of coronary spasm; adequate early stent implantation may prevent AMI [4,6]. Demonstration of non-calcified mild to moderate atherosclerotic plaque by IVUS may assist in determining the indications for treatment. Risk factors such as smoking and hypercholesterolemia should be strictly controlled when occult atherosclerosis is detected by IVUS [9]. Coronary spasm has been known to accelerate the progression of atherosclerosis, and preexisting atherosclerosis is one of the most important determinant factors of the long-term prognosis [4].

Although cases such as ours are rare, coronary artery spasm should be considered when chest symptoms recur after successful coronary interventions. Full-dose nitrate and calcium antagonists are necessary if the ergonovine provocative test is positive.

References

[1] Sueda S, Kohno H, Fukuda H, et al. Frequency of provoked coronary spasms in patients undergoing coronary arteriography using a spasm provocation test via intracoronary administration of ergonovine. Angiology 2004;55:403–11.
[2] Saito S, Yamagishi M, Takayama T, et al. Plaque morphology at coronary sites with focal spasm in variant angina: study using intravascular ultrasound. Circ J 2003;67:1041–5.
[3] Hwan Han S, Kon Koh K, Jin Oh K, Hyun Yoon K. Unstable angina complicated by vasospasm and intracoronary thrombus and no evidence of plaque rupture. Int J Cardiol 2006;111:329–32.
[4] Sosnowski C, Dabrowski R, Wiernikowski A, Rewicki M, Ruzyllo W. Coronary artery stent placement as a treatment of acute coronary

Please cite this article as: Yuxin Li et al., Generalized spasm of the right coronary artery after successful stent implantation provoked by intracoronary administration of ergonovine, International Journal of Cardiology (2006), doi:10.1016/j.ijcard.2006.07.137

syndrome in course of variant angina. Int J Cardiol Apr 4 2006;108 (2):259–61.
[5] Cheng TO. Ergonovine test for coronary artery spasm. Int J Cardiol Mar 13 2006 [Electronic publication ahead of print].
[6] Adlam D, Azeem T, Ali T, Gershlick A. Is there a role for provocation testing to diagnose coronary artery spasm? Int J Cardiol Jun 22 2005;102(1):1–7.
[7] Yamagishi M, Ito K, Tsutsui H, et al. Lesion severity and hypercholesterolemia determine long-term prognosis of vasospastic angina treated with calcium channel antagonists. Circ J 2003;67:1029–35.
[8] Kugiyama K, Yasue H, Okumura K, et al. Nitric oxide activity is deficient in spasm arteries of patients with coronary spastic angina. Circulation 1996;94:266–71.
[9] Nobuyoshi M, Tanaka M, Nosaka H, et al. Progression of coronary atherosclerosis: is coronary spasm related to progression? J Am Coll Cardiol 1991;18:904–10.

Please cite this article as: Yuxin Li et al., Generalized spasm of the right coronary artery after successful stent implantation provoked by intracoronary administration of ergonovine, International Journal of Cardiology (2006), doi:10.1016/j.ijcard.2006.07.137

Heart Vessels (2006) 21:135–136
DOI 10.1007/s00380-005-0860-6

GRAPHIC REPORT

**Yuichi Sato · Makoto Ichikawa · Kanae Nakanishi
Naoya Matsumoto · Shunichi Yoda · Yuji Kasamaki
Tadateru Takayama · Yasushi Koyama · Fumio Inoue
Motoichiro Takahashi · Takahisa Uchiyama · Satoshi Saito**

Multidetector computed tomography of a saphenous vein graft aneurysm

Received: May 24, 2005 / Accepted: July 23, 2005

Key words Multidetector computed tomography · Saphenous vein graft aneurysm

A 64-year-old man with a history of hypercholesterolemia, smoking, arteriosclerosis obliterans, and aortocoronary bypass grafting (CABG) presented with an enlarging right cardiophrenic angle mass found on routine chest X-ray (Fig. 1). At the time of his CABG 14 years earlier, the left internal mammary artery was used to graft the left anterior descending artery and the saphenous vein graft (SVG) was placed to the right coronary artery. He had a long-standing history of hypercholesterolemia. Multidetector computed tomography (MDCT) was performed using an Aquillion 16 (16-detector-row, Toshiba Medical, Tokyo, Japan). The scan protocol and image reconstruction method have been reported previously.[1–4] The reconstructed data were transferred to a computer workstation (M 900 quadra; AMIN, Tokyo, Japan) for processing of the surface volume rendering and multiplanar reformation images. The volume-rendering images (Fig. 2A,B) showed an aneurysm of the saphenous vein graft with a thick, low attenuation suggesting a thrombus. The native right coronary artery was totally occluded. The SVG–right coronary artery and left internal mammary artery–left descending artery grafts were patent. The multiplanar reformation image also showed a markedly dilated SVG (Fig. 2C). The short-axis image at the level of the maximum SVG dilatation (Fig. 2D) showed that the diameter of the SVG was 37 × 35 mm. The SVG aneurysm contained a thrombus and eccentric coronary artery lumen, and it compressed the right atrium. Conventional coronary angiography also demonstrated a tortuously dilated SVG graft but failed to show associated thrombus. With hesitation to carry out surgical treatment, the patient was maintained on oral anticoagulant therapy uneventfully.

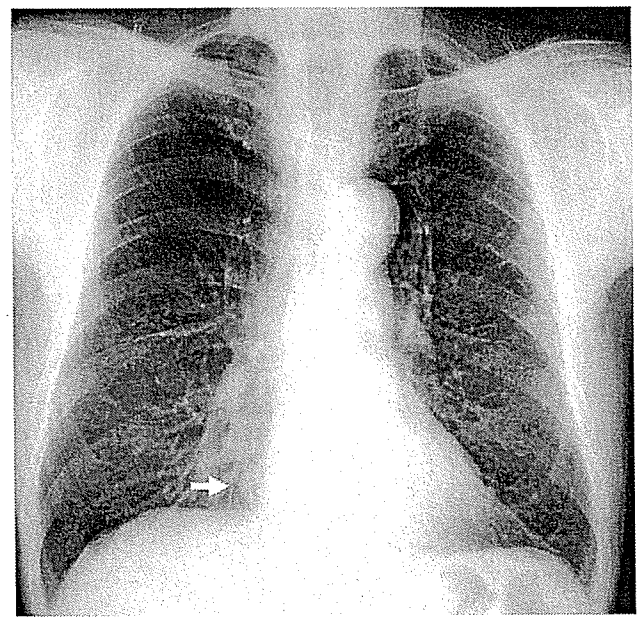

Fig. 1. Chest X-ray reveals a right cardiophrenic angle mass (*arrow*)

Saphenous vein graft aneurysm after CABG is a rare condition. There are approximately 70 cases reported in the literature. The mechanism of SVG aneurysm formation is uncertain, but it is frequently associated with atherosclerosis and hyperlipidemia.[5,6] Patients with SVG aneurysm are usually asymptomatic,[7] but are in a potentially fatal situation, since SVG aneurysms may develop myocardial ischemia due to occlusion and periodic emboli,[8] and rupture.[9] In asymptomatic patients, an abnormal mass detected on

Y. Sato (✉) · M. Ichikawa · K. Nakanishi · N. Matsumoto · S. Yoda · Y. Kasamaki · T. Takayama · T. Uchiyama · S. Saito
Department of Cardiology, Nihon University School of Medicine, 1-8-13 Kanda-Surugadai, Chiyoda-ku, Tokyo 101-8309, Japan
Tel. +81-3293-1711; Fax +81-3295-1859
e-mail: yuichis@med.nihon-u.ac.jp

Y. Koyama
Division of Advanced Cardiac Imaging, Department of Cardiology, Cleveland Clinic Foundation, Cleveland, OH, USA

F. Inoue · M. Takahashi
Department of Radiology, Nihon University School of Medicine, Tokyo, Japan

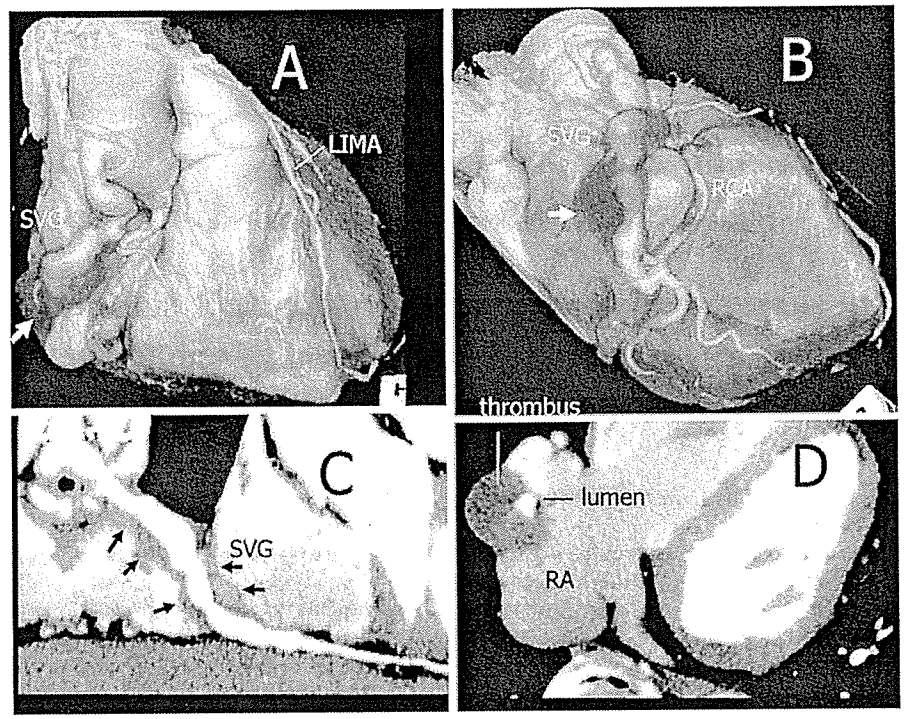

Fig. 2. **A** Right anterior oblique view of the volume-rendering image showing a tortuously dilated saphenous vein graft (*SVG*) with a low-attenuation mass suggesting a thrombus (*arrow*). The left internal mammary artery (*LIMA*) – left anterior descending artery (*LAD*) graft is patent. **B** Bottom view of the volume-rendering image shows a dilated SVG (*arrow*) and the patent SVG – right coronary artery (*RCA*). **C** Curved multiplanar reformation image illustrates a diffuse thrombus (*arrows*) along the RCA. **D** Axial image shows that the SVG aneurysm contains laminated thrombus and eccentric, contrast-filled lumen. *RA*, right atrium

chest X-ray usually leads to a further workup and correct diagnosis.[7] Echocardiography is capable of detecting large SVG aneurysms, but visualization of the whole SVG is not possible. With its high spatial resolution, MDCT can become the first choice of diagnostic modality because it permits the accurate measurement of the size of the aneurysm and the detection of thrombus. The long-term prognosis and treatment for asymptomatic patients with SVG aneurysms are uncertain since a large-scale clinical trial is unavailable because of the low incidence. However, in a small series of patients ($n = 11$), Dieter et al.[10] have reported no survival advantage with an early aggressive interventional approach. In conclusion, MDCT has the potential to be the standard diagnostic tool for the evaluation of SVG aneurysm after CABG.

References

1. Sato Y, Kanmatsuse K, Inoue F, Horie T, Kato M, Kusama J, Yoshimura A, Imazeki T, Furuhashi S, Takahashi M (2003) Noninvasive coronary artery imaging by means of multislice spiral computed tomography: a novel approach for retrospectively ECG-gated reconstruction technique. Circ J 67:107–111
2. Sato Y, Inoue F, Yoshimura A, Fukui T, Imazeki T, Kato M, Ono H, Yoda S, Mitsui M, Matsumoto N, Furuhashi S, Takahashi M, Kanmatsuse K (2003) Regression of an atherosclerotic coronary artery plaque demonstrated by multislice spiral computed tomography in a patient with stable angina pectoris. Heart Vessels 18:224–226
3. Sato Y, Mitsui M, Takahashi H, Miyazawa T, Okabe H, Inoue F, Kusama J, Horie T, Matsumoto N, Hori Y, Furuhashi S, Takahashi M, Kanmatsuse K (2004) A giant left circumflex coronary artery-right atrium arteriovenous fistula detected by multislice spiral computed tomography. Heart Vessels 19:55–56
4. Sato Y, Matsumoto N, Inoue F, Imazeki T, Kusama J, Tamaki T, Furuhashi S, Takahashi M, Kanamaru H, Karasawa K, Ayusawa M, Harada K, Kanmatsuse K (2004) Assessment of coronary artery abnormalities in a patient with Kawasaki disease by multislice computed tomography. Heart Vessels 19:297–299
5. Liang BT, Antman EM, Taus R, Collins JJ Jr, Schoen FJ (1988) Atherosclerotic aneurysms of aortocoronary vein grafts. Am J Cardiol 61:185–188
6. Teja K, Dillingham R, Mentzer RM (1987) Saphenous vein aneurysms after aorotocoronary bypass grafting: postoperative internal and hyperlipidemia as determining factors. Am Heart J 113:1527–1529
7. Wight JN, Salem D, Vannan MA, Pandian NG, Bankoff M, Rozansky MI, Semple JP, Dohan MC (1997) Asymptomatic large coronary artery saphenous vein bypass graft aneurysm: a case report and review of the literature. Am Heart J 133:454–460
8. Taliercio CP, Smith HC, Pluth JR, Gibbons RJ (1986) Coronary artery venous bypass graft aneurysm with symptomatic coronary artery emboli. J Am Coll Cardiol 7:435–437
9. Bramlet DA, Behar VS, Ideker RE (1982) Aneurysm of a saphenous vein bypass graft associated with aneurysm of native coronary arteries. Catheter Cardiovasc Diagn 8:489–494
10. Dieter RS, Patel AK, Yandow D, Pacanowski JP, Bhattacharya A, Gimelli G, Kosolcharoen P, Russell D (2003) Conservative vs. invasive treatment of aortocoronary saphenous vein graft aneurysms: treatment algorithm based upon a large series. Cardiovasc Surg 11:507–513

Heart Vessels (2005) 20:298–300
DOI 10.1007/s00380-005-0826-8

GRAPHIC REPORT

Yuichi Sato · Fumio Inoue · Taeko Kunimasa
Naoya Matsumoto · Shunichi Yoda · Shigemasa Tani
Tadateru Takayama · Takahisa Uchiyama
Hiroshi Tanaka · Satoru Furuhashi · Motoichiro Takahashi
Yasushi Koyama · Satoshi Saito

Diagnosis of anomalous origin of the right coronary artery using multislice computed tomography: evaluation of possible causes of myocardial ischemia

Received: October 4, 2004 / Accepted: January 29, 2005

Abstract Anomalous origin of the right coronary artery (RCA) is a rare condition, but may cause myocardial ischemia and sudden death. Multislice computed tomography, which allows three-dimensional visualization of the coronary artery with high spatial resolution, may be the most promising imaging modality for diagnosing this anomaly. We describe a patient with anomalous origin of the RCA arising from the left sinus of Valsalva. Volume rendering, and axial and curved multiplanar images showed stenosis in the proximal portion of the RCA that coursed between the aorta and the pulmonary artery, and an acute angled take-off of the RCA from the aorta. Three-dimensional virtual angioscopic images showed a hypoplastic RCA orifice and luminal narrowing in the proximal portion of the RCA. Multislice computed tomography was thought to be useful for detecting anomalous origin of the RCA and for evaluating possible causes of myocardial ischemia.

Key words Multislice computed tomography · Anomalous origin of coronary artery · Virtual angioscopy

Introduction

Anomalous origin of the right coronary artery (RCA) from the left sinus of Valsalva is a rare congenital anomaly with an incidence ranging from 0.03% to 0.71%.[1–4] Nonfatal or fatal acute myocardial infarction[5] and sudden death[6] occur in such patients, most notably in young athletes.[7,8] We describe a patient in whom multislice computed tomography (MSCT) was useful for identifying anomalous origin of the RCA. Three-dimensional virtual coronary angioscopy showed a hypoplastic RCA orifice and narrowing of the proximal portion of the RCA, which coursed between the aorta and the pulmonary artery. These findings suggest possible causes of exercise-induced myocardial ischemia.

Y. Sato (✉) · F. Inoue · T. Kunimasa · N. Matsumoto · S. Yoda · S. Tani · T. Takayama · T. Uchiyama · S. Saito
Department of Cardiology, Nihon University School of Medicine, 1-8-13 Kanda-Surugadai, Chiyoda-ku, Tokyo 101-8309, Japan
Tel. +81-3-3293-1711; Fax +81-3-3295-1859
e-mail: yuichis@med.nihon-u.ac.jp

H. Tanaka · S. Furuhashi · M. Takahashi
Department of Radiology, Nihon University School of Medicine, Tokyo, Japan

Y. Koyama
Department of Cardiology, Cleveland Clinic Foundation, Cleveland, OH, USA

Case report

A 71-year-old woman underwent MSCT coronary angiography because of oppression of the chest on effort. She had no previous history suggesting myocardial ischemia or coronary risk factors, such as hypercholesterolemia, diabetes mellitus, hypertension, or smoking. Exercise myocardial perfusion single-photon emission computed tomography (SPECT) using a rest ^{201}thallium/stress ^{99m}Tc-tetrofosmin dual-isotope, separate acquisition protocol revealed a reversible perfusion defect on the inferior myocardial segments. Multislice computed tomographic coronary angiography was performed using a Somatom Volume Zoom (4-detector-row; Siemens, Nuremberg, Germany) with a collimation of 1.0 mm; table feed, 1.5 mm/rotation; 140 kV; 320 mA; and gantry rotation time, 500 ms. Our scan protocol and image reconstruction method have been reported previously.[9–11] Metoprolol (40 mg) was given 90 min prior to the scan in order to reduce the heart rate to perform the single-phase algorithm. Following determination of the contrast transit time from the cubital vein to the ascending aorta by injection of 15 ml of nonionic contrast medium (Iomeron 350 100-ml syringe; Eisai, Tokyo, Japan), the remaining contrast medium (85 ml) was injected at a speed of 2.8 ml/s. Image reconstruction was made with a reconstruction window (250 ms) positioned immediately before the atrial contraction period, which could be recognized by the peak of the P wave on the monitor ECG. The reconstructed data were transferred to a computer workstation (3D Vir-

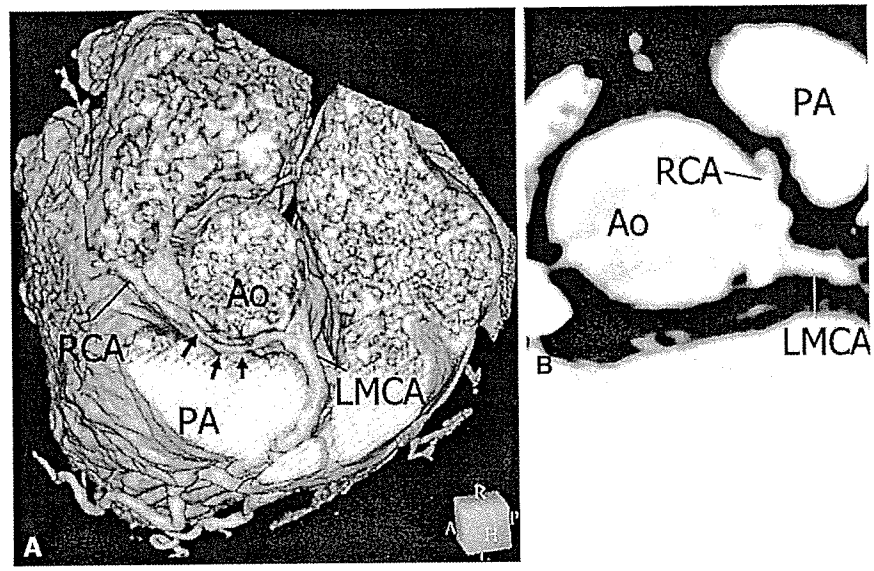

Fig. 1. **A** Volume-rendering image showing the anomalous origin of the right coronary artery (*RCA*), which arises from the left sinus of Valsalva, separately from the left main coronary artery (*LMCA*). **B** The proximal portion of the RCA is narrowed and courses between the aorta (*Ao*) and the pulmonary artery (*PA*)

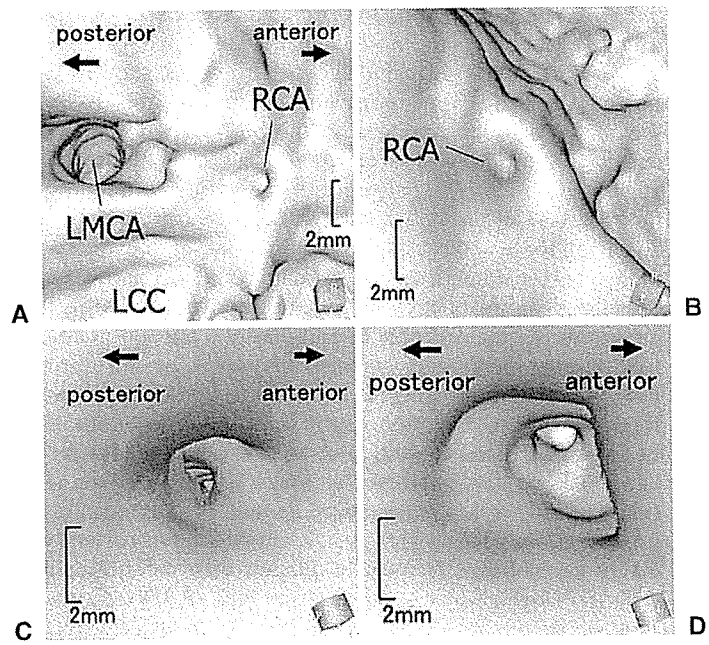

Fig. 2. **A** Three-dimensional virtual angioscopic image of the left sinus of Valsalva showing a small orifice of the right coronary artery (*RCA*) as compared to the orifice of the left main coronary artery (*LMCA*). *LCC*, left coronary cusp. **B** Magnified view of the RCA orifice. **C** The view into the distal side of the RCA showing the slit-like appearance of the RCA lumen. **D** The view from the portion distal to the stenotic lumen

tuoso; Siemens) to process surface volume-rendering, and curved multiplanar reformation images. The three-dimensional (3D) virtual coronary angioscopic images were created by another 3D workstation (Real Intage; KGT, Tokyo, Japan).

The volume-rendering image (Fig. 1A) showed that the RCA arose from the left sinus of Valsalva with an acute angle, and coursed anteriorly between the aortic root and the pulmonary artery to enter the right atrioventricular groove. The proximal portion of the RCA was significantly narrowed as compared to the distal portion. The axial image (Fig. 1B) showed an acute angled take-off of the RCA from the left sinus of Valsalva, separate from the left main coronary artery. Three-dimensional virtual angioscopic images (Fig. 2) demonstrated that both the left main coronary artery and the RCA arose separately from the left sinus of Valsalva (Fig. 2A). The orifice of the RCA was hypoplastic (Fig. 2B). The proximal portion (8–15 mm from the orifice) of the RCA was stenotic (Fig. 2C). Beyond this portion, the luminal size became normal (Fig. 2D).

The patient refused conventional coronary angiography and medical treatment with β-blocker was initiated. She became free from chest pain and the second myocardial perfusion SPECT under medication revealed a negative test result.

Discussion

Anomalous origin of the RCA is a rare condition, but it has clinical importance because nonfatal or fatal myocardial infarction and sudden death occur in up to 30% of the patients.[12] In the majority of patients, the RCA courses between the aortic root and the pulmonary artery[4] as documented in our patient. The causes of myocardial ischemia remain unclear, but the acute-angle take-off and kinking of the RCA as it arises from the aorta, the flap-like closure of the abnormal coronary orifice, compression of the RCA between the aorta and the pulmonary artery, and spasm of the anomalous RCA have been thought to be possible mechanisms.[6–8] In our patient, MSCT demonstrated a small RCA orifice, the acute angle take-off of the RCA from the aorta, and stenosis of the proximal RCA segment as it coursed between the aorta and the pulmonary artery. Three-dimensional virtual angioscopic images showed a small RCA orifice and narrowing of the proximal RCA segment which corresponded to the portion between the aorta and the pulmonary artery. The accuracy of 3D virtual angioscopy in detecting significant stenosis determined by intravascular ultrasound has been described previously.[13] Although these findings suggest possible causes of exercise-induced myocardial ischemia, our data could not clarify the exact mechanism of myocardial ischemia because MSCT images were obtained only in end-diastole, but not in systole during which compression of the RCA by the great vessels might have occurred. In addition, the flap-like texture of the RCA orifice might have been overlooked because the spatial resolution of MSCT was limited. Conventional coronary angiography, which is still a domain in the diagnosis of coronary artery anomalies, was not performed in our patient. However, identification of coronary artery anomalies is frequently difficult with conventional coronary angiography because of the lack of 3D information which relates the course of the RCA to the great vessels.[14] Magnetic resonance imaging is an alternative, noninvasive imaging modality that is capable of detecting coronary anomalies.[15,16] Future development of MSCT hardware should provide higher spatial resolution and allow motion analysis during the whole cardiac cycle, and would be more informative for the evaluation of the mechanisms by which myocardial ischemia is provoked in patients with anomalous origin of the RCA.

References

1. Alexander RW, Griffith GC (1956) Anomalies of the coronary arteries and their clinical significance. Circulation 14:800–805
2. Engel HJ, Torres C, Page HL (1975) Major variations in anatomical origin of the coronary arteries: angiographic observations in 4250 patients without associated congenital heart disease. Cathet Cardiovasc Diagn 1:157–169
3. Kimbiris D, Abdulmassih SI, Segal BL, Bemis CE (1978) Anomalous aortic origin of coronary arteries. Circulation 58:606–615
4. Yamanaka O, Hobbs RE (1990) Coronary artery anomalies in 126,595 patients undergoing coronary angiography. Cathet Cardiovasc Diagn 21:28–40
5. Kaku B, Kanaya H, Ikeda M, Uno Y, Fujita S, Kato F, Oka T (2000) Acute inferior myocardial infarction and coronary artery spasm in a patient with an anomalous origin of the right coronary artery from the left sinus of Valsalva. Jpn Circ J 64:641–643
6. Benge W, Martins JB, Funk DC (1980) Morbidity associated with anomalous origin of the right coronary artery from the left sinus of Valsalva. Am Heart J 99:96–100
7. Maron BJ, Epstein SE, Roberts WC (1986) Sudden death in young competitive athletes. J Am Coll Cardiol 7:204–214
8. Basso C, Maron BJ, Corrado D, Thiene G (2000) Clinical profile of congenital coronary artery anomalies with origin from the wrong aortic sinus leading to sudden death in young competitive athletes. J Am Coll Cardiol 35:1493–1501
9. Sato Y, Kanmatsuse K, Inoue F, Horie T, Kato M, Kusama J, Yoshimura A, Imazeki T, Furuhashi S, Takahashi M (2003) Noninvasive coronary artery imaging by means of multislice computed tomography: a novel approach for retrospectively ECG-gated reconstruction technique. Circ J 67:107–111
10. Sato Y, Inoue F, Yoshimura A, Fukui T, Imazeki T, Kato M, Ono H, Yoda S, Mitsui M, Matsumoto N, Furuhashi S, Takahashi M, Kanmatsuse K (2003) Regression of an atherosclerotic coronary artery plaque demonstrated by multislice computed tomography in a patient with stable angina pectoris. Heart Vessels 18: 224–226
11. Sato Y, Mitsui M, Takahashi S, Miyazawa T, Okabe H, Inoue F, Kusama J, Horie T, Matsumoto N, Hori Y, Furuhashi S, Takahashi M, Kanmatsuse K (2003) A giant left circumflex coronary artery-right atrium arteriovenous fistula detected by multislice computed tomography. Heart Vessels 19:55–56
12. Roberts WC, Siegel RJ, Zipes DP (1982) Origin of the right coronary artery from the left sinus of Valsalva and its functional consequences: analysis of 10 necropsy patients. Am J Cardiol 49: 863–868
13. Schroeder S, Kopp AF, Ohnesorge B, Loke-Gie H, Baumbach A, Herdeg C, Claussen CD, Karsh KR (2002) Virtual coronary angioscopy using multislice computed tomography. Heart 87:205–209
14. Serota H, Barth C, Seucy CA, Vandormael M, Aguirre F, Kern M (1990) Rapid identification of the course of anomalous coronary arteries in adults: the "dot and eye" method. Am J Cardiol 65:891–898
15. Taylor AM, Thorne SA, Rubens MB, Jhooti P, Keegan J, Gatehouse PD, Wiesmann F, Grothues F, Somerville J, Pennel DJ (2000) Coronary artery imaging in grown up congenital heart disease: complementary role of magnetic resonance and X-ray coronary angiography. Circulation 101:1670–1678
16. Bunce NH, Lorenz CH, Keegan J, Reyes EM, Firmin DN, Pennell DJ (2003) Coronary artery anomalies: assessment with free-breathing three-dimensional coronary MR angiography. Radiology 227:201–208